AD A055936

FOR FURTHER TRAN

DGW
15881
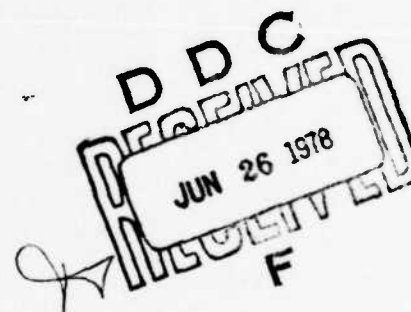
EPITAXIAL GROWTH OF SEMI-INSULATING GaAs

S. T. Jolly, D. S. Yaney, and S. Y. Narayan
RCA Laboratories
Princeton, New Jersey 08540

DDC FILE COPY

MARCH 1978

DDC
JUN 26 1978
F

SEMIANNUAL REPORT
for period 1 July 1977 to 31 December 1977

78 06 23 099

REPORT DOCUMENTATION PAGE	READ INSTRUCTIONS BEFORE COMPLETING FORM	
1. REPORT NUMBER	2. GOVT ACCESSION NO.	3. RECIPIENT'S CATALOG NUMBER
4. TITLE (and Subtitle) EPITAXIAL GROWTH OF SEMI-INSULATING GaAs	5. TYPE OF REPORT & PERIOD COVERED Semiannual Report (1 Jul 1977 — 31 Dec. 1977)	
	6. PERFORMING ORG. REPORT NUMBER PRRL-78-CR-10	
7. AUTHOR(s) S. T. Jolly, D. S. Yaney, and S. Y. Narayan	8. CONTRACT OR GRANT NUMBER(s) DARPA Order No. 3441 BASIC Program Code 7D10 N00014-77-C-0542	
9. PERFORMING ORGANIZATION NAME AND ADDRESS RCA Laboratories Princeton, New Jersey 08540	10. PROGRAM ELEMENT, PROJECT, TASK AREA & WORK UNIT NUMBERS PE 61101E/Program Code 7D10/NR 243-018	
11. CONTROLLING OFFICE NAME AND ADDRESS Defense Advanced Research Projects Agency (DOD) 1400 Wilson Boulevard Arlington, Virginia 22209	12. REPORT DATE March 1978	
	13. NUMBER OF PAGES 28 P.	
14. MONITORING AGENCY NAME & ADDRESS (If different from Controlling Office) Office of Naval Research Arlington, Virginia 22217	15. SECURITY CLASS. (of this report) Unclassified	
	15a. DECLASSIFICATION/DOWNGRADING SCHEDULE N/A	

16. DISTRIBUTION STATEMENT (of this Report)

Approved for public release; distribution unlimited.

17. DISTRIBUTION STATEMENT (of the abstract entered in Block 20, if different from Report)

JUN 26 1978

18. SUPPLEMENTARY NOTES

ONR Scientific Officer
Telephone: (202) 696-4218

19. KEY WORDS (Continue on reverse side if necessary and identify by block number)

Semi-insulating (SI) GaAs	Chromium doping
Epitaxial growth	Buffer layers
Photoconductive (PC) response	Photoelectronic methods

20. ABSTRACT (Continue on reverse side if necessary and identify by block number)

This report describes the progress during the first six months of a 12-month research program to develop techniques for the epitaxial growth of high-resistivity GaAs layers. These high-resistivity layers will be evaluated as buffer layers for planar GaAs devices such as field-effect transistors (FETs) and transferred-electron logic devices (TELDs).
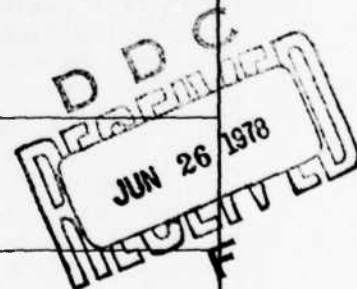
DD FORM 1473
1 JAN 73

299 000   hc

20.

A modified version of the standard AsH_3/Ga/HCl/H_2 vapor-phase reactor and its associated gas-handling system was designed and constructed. The new design allows easy in situ vapor etching of the reactor tube before every growth run. Provision for Cr-doping using a CrO_2Cl_2/He mixture was included. The reactor has built-in flexibility to allow experiments with a solid Cr-source.

Both undoped and Cr-doped epitaxial layers with resistivity in excess of 10^5 ohm-cm were grown. The point-contact-breakdown voltage of both types of layers was in excess of 1500 V. Several FET wafers with both undoped and Cr-doped buffer layers were grown for evaluation. The surface morphology of the Cr-doped layers was excellent.

Methods for the characterization of both semi-insulating (SI) GaAs substrates and SI GaAs epitaxial layers were explored. A major problem in characterizing epitaxial SI GaAs layers grown on SI substrates is that the effect of the epitaxial layer cannot be resolved from that of the substrate. Room-temperature photoconductivity measurements show that a peak in the response at about 0.9 eV is the signature of Cr presence in the lattice. We conclude that photoconductivity measurements can be used to nondestructively detect the presence of Cr in GaAs. It is likely that other deep states could be resolved by extending the measurement to lower temperatures and photon energies. Application of this method directly to the in situ detection of Cr in thin epi layers grown on SI GaAs substrates is not straightforward, however. Measurements of the optical-absorption coefficient of Cr-doped material showed a negligible increase at 0.9 eV. Thus, the material remains optically transparent, and any increase in photoconductivity could come from the Cr-doped substrate as well as the buffer layer. In view of the relative thickness, it seems unlikely that the effects of the buffer layer at 0.9 eV would be seen at all.

On the other hand, band-edge illumination is absorbed very rapidly with depth because of the large value of the absorption coefficient. Behavior of the PC spectral response for the substrates tested was always similar. Conduction increased near the band edge and then dropped off as the photon energy increased. This is interpreted as being due to a large value of the surface recombination velocity S. As the generated hole-electron pairs are confined to the surface, the photoconductivity is seen to decrease. With SI epi films on SI substrates, the characteristic dip above the band edge seen for the substrates was not observed, indicating a lower value of S in the epi material.

The usefulness of photoelectronic measurements with subgap and bandgap radiation in characterizing GaAs:Cr has become apparent. Future effort will be directed toward lowering measurement temperatures for a better resolution of deep levels.

PREFACE

This semiannual report describes research done in the Microwave
Technology Center of RCA Laboratories during the period 1 July 1977
to 31 December 1977 in a program sponsored by Defense Advanced Research
Projects Agency (DOD) under DARPA Order No. 3441 BASIC and monitored by the
Office of Naval Research under Contract No. N00014-77-C-0542. F. Sterzer is
the Center's Director; S. Y. Narayan is the Project Supervisor and S. T. Jolly
is the Project Scientist. D. S. Yaney and D. R. Capewell also participated
in the research project.

ACCESSION for

NTIS   White Section
DDC   Buff Section   ☐
UNANNOUNCED ☐
JUSTIFICATION

BY
DISTRIBUTION/AVAILABILITY CODES

Dist.

78 06 23 099

TABLE OF CONTENTS

LIST OF ILLUSTRATIONS

LIST OF TABLES

SECTION I

INTRODUCTION

The objective of this program is to develop techniques for the vapor-phase growth of high-resistivity epitaxial layers of gallium arsenide on semi-insulating gallium arsenide substrates. A capability to grow such layers of high-quality material with minimum structural defects and good surface quality for use as buffer layers prior to the growth of active layers for such devices as FETs and TELDs will eliminate the device performance problems caused by poor and inconsistent substrate quality.

During the first quarter, a vapor-phase GaAs reactor and its associate gas handling system were designed and constructed. Preliminary test runs were performed to check system operation under normal operating conditions. In the second quarter, both undoped and Cr-doped high-resistivity GaAs epitaxial layers were grown. The surface morphology of the high-resistivity layers was excellent.

During the second quarter, ~~we began~~ the investigation of a number of techniques, in order to develop a capability for characterizing both substrate material and high-resistivity epitaxial layers. This report will describe ~~our~~ progress in all of these areas.

SECTION II

MATERIAL GROWTH

A. INTRODUCTION

The success of planar devices such as GaAs field-effect transistors (FETs) and transferred-electron logic devices (TELDs) depends on the capability of growing thin (≤ 1.5 μm) high-quality n layers on substrates which are "inert" (i.e., they do not affect the electrical and mechanical properties of thin layers grown epitaxially on them). A major problem is the present unreliability of available substrate material. A possible solution which this program proposes to investigate is the growth of a high-quality semi-insulating buffer layer with good surface morphology, high electrical resistivity, and the minimum of interaction with the active n layer subsequently grown on it.

In a previous company-sponsored effort, we have established the feasibility of the epitaxial growth of chromium-doped semi-insulating (SI) GaAs, using CrO_2Cl_2. This study established the following points:

1. For chromium doping with CrO_2Cl_2 to be effective, the background donor density in the reactor must be $\leq 2 \times 10^{15} cm^{-3}$.

2. When the background donor density is in the required range, chromium-doped SI GaAs layers can be grown. The point-contact-breakdown voltage of such epi-SI GaAs layers is in excess of 1500 V. Measurements carried out on these layers at the USAF Avionics Laboratory indicate a resistivity in the 10^6-10^7-ohm-cm range.

3. The surface morphology of the chromium-doped epi layers was poor compared to that of epi n layers. The reason for this poor morphology is not well understood. Careful adjustment of the CrO_2Cl_2 gas flow resulted in some minor improvement.

4. The CrO_2Cl_2/H_2 dopant mixture decomposed in the feed tube, and the deposit clogged the tube. It was suspected that the H_2 in the mixture reduced CrO_2Cl_2 in the hot part of the feed tube.

5. The 500-ppm CrO_2Cl_2/H_2 mixture was then replaced by a 500-ppm CrO_2Cl_2/He mixture. This greatly minimized the decomposition in the feed tube. Furthermore, lower flow rates of the CrO_2Cl_2/He mixtures could be used

to obtain SI GaAs. The surface quality also improved slightly. The point-contact breakdown of the grown layers was again in excess of 1500 V.

One chromium-doped epitaxial GaAs layer was evaluated at the USAF Avionics Laboratory, Dayton, Ohio. In one experiment, a (100) oriented slice from a bulk-grown SI GaAs substrate was cut into two pieces. On one, a 5-μm-thick epitaxial chrome-doped layer was grown, and the other was used as a control sample. At the Avionics Laboratory, the electron-and-hole concentration, mobility, and IR photoconductivity at 4.2 K were measured. Table 1 and Fig. 1 illustrate the results. The superior properties of the epi-SI layer are evident. The resistivity of the epi layer is 10^7 ohm-cm. Figure 1 shows that the photoconductive response of the epi layer is much sharper than that of the substrate. This is believed to be indicative of superior crystal quality.

In the final analysis, the best measure of material quality is the performance of an active device fabricated from it. n^+-n-n_B(Buffer)-SI GaAs wafers were grown in situ for power FET fabrication; n_B denotes an epitaxial SI GaAs buffer layer. The buffer-layer thickness was about 5 μm. FETs of 1.5-μm gate length were fabricated from this wafer. Table 2 summarizes the results obtained. *Note that excellent performance was obtained from a FET with* 1.5-μm *gate length at frequencies as high as 22 GHz* [1]. These data indicate that the n layer grown on an epi-SI buffer layer has excellent electron-drift mobility. These results are far superior to those obtained from 0.8-μm-gate FETs fabricated from n layers grown directly on bulk-grown SI GaAs substrates.

We have also fabricated planar transferred-electron logic devices (TELDs) from a wafer with an epitaxial SI GaAs buffer layer. Post-threshold current drops as high as 28% were obtained with three terminal TELDs; this, again, is indicative of higher electron-drift mobility in n layers grown on epitaxial SI GaAs layers.

While the feasibility of growth of SI GaAs layers by vapor-phase epitaxy (VPE) and its impact on planar GaAs devices has been established, further research work is necessary.

1. For the improvement of surface morphology, the occurrence of microscopic pitlike defects must be eliminated. This is necessary to obtain submicron line lengths and features required for microwave and multigigabit-rate logic circuits. The reasons for the occurrence of these imperfections is not understood.

3

TABLE 1

Data Taken by USAF Avionics Laboratory, Dayton, Ohio

	Type	Resistivity (ohm-cm)	$n\text{-cm}^{-3}$	$p\text{-cm}^{-3}$	μ_n $(cm^2/V\cdot s)$	μ_p $(cm^2/V\cdot s)$
Substrate	n	7.11×10^7			1041	
Epitaxial buffer layer	n	7.09×10^7	1.65×10^7	1.58×10^8	4202	403

TABLE 2

RCA GaAs FET Performance (with chrome-doped buffer layer)

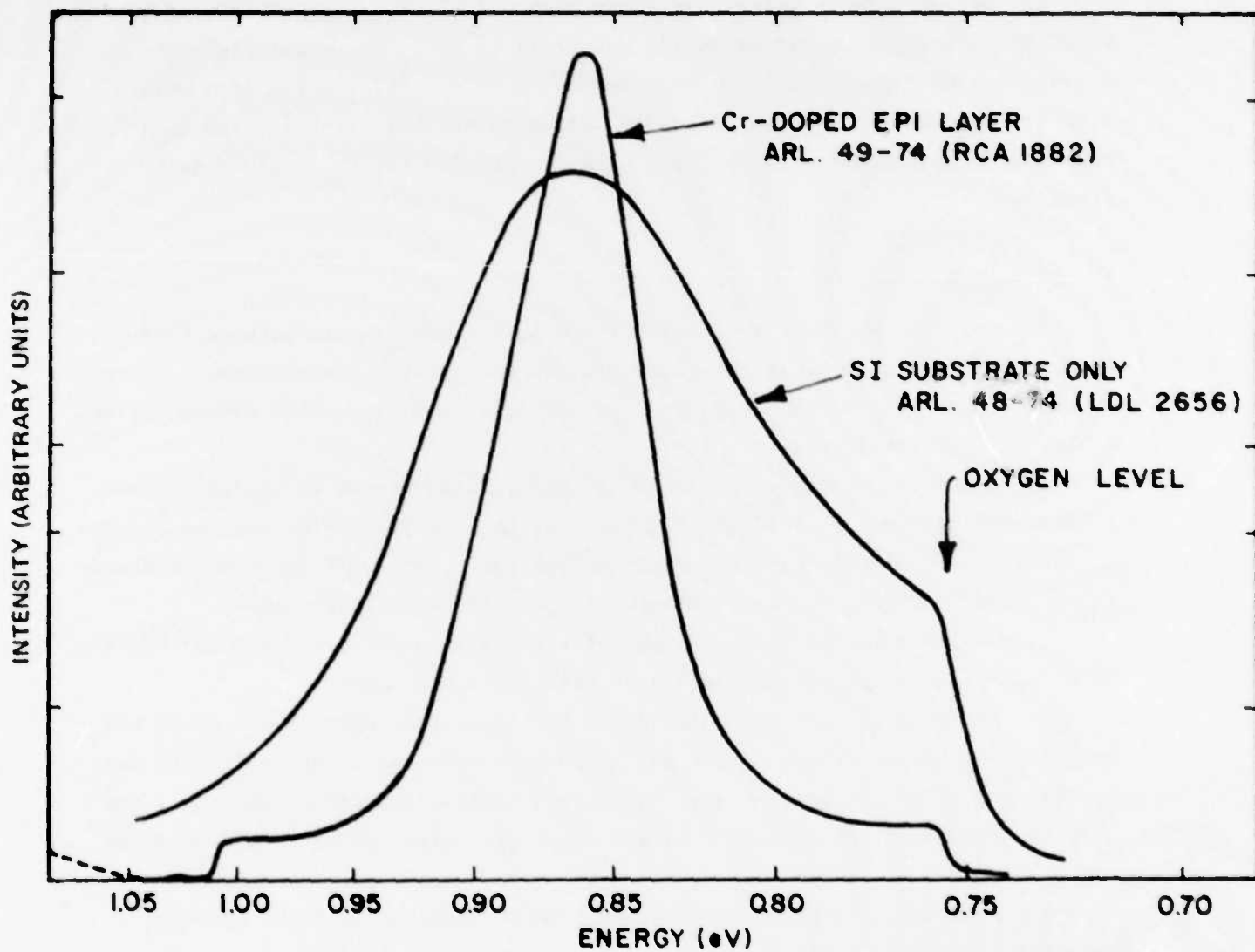| Frequency (GHz)	Linear Gain (dB)	Output Power (mW)	Gain at P_{out} (dB)	Power-Added Efficiency (%)	Operating Condition (Source Periphery)
9	5.5	1000	4.3	16.3	Class A (1800 µm)
15	6.7	451	5.2	12.5	Class A (1200 µm)
18	6.3	225	4.5	5.4	Class A (1200 µm)
21	5	186	4.3	11.9	Class A (600 µm)
22	5.6	141	4.8	9	Class A (600 µm)

4

Figure 1. Photoconductivity response of bulk Cr-doped substrate and epitaxial Cr-doped buffer layer. Measurement made at AFAL, Dayton, Ohio.

2. Optimum conditions for reproducible and repeatable growth of SI
GaAs layers have to be established.

3. The use of metallic Cr and its transport by Cl_2 gas may eliminate
the need for CrO_2Cl_2, which is highly toxic. This needs to be investigated.

4. Researchers at Fujitsu in Japan have established that the use of
metallic Fe and its transport to the substrate as $FeCl_2$ can result in high-
resistivity Fe-doped GaAs [2]. They report excellent FET results from wafers
with Fe-doped buffer layers. Fe-doped GaAs with resistivities as high as 10^5
ohm-cm have been achieved. Fe-doped high-resistivity layers should also be
studied.

B. REACTOR DESCRIPTION

The vapor-phase reactor in which the original experiments were carried
out was modified to make it more suitable for this particular program. Figure 2
shows the schematic of the redesigned gas-handling system. This system has the
following characteristics:

1. Ability to operate as a "normal" $Ga/Cl_2/AsH_3$ system employing palladi-
um-diffused hydrogen as the diluting gas. It is also planned to add the ability
to substitute ultrapure nitrogen for the hydrogen. This will be of significance
in attempts to employ metallic chromium or iron as the doping element.

2. Addition to the reactor input of a third input line for the introduction
of a chromyl chloride/helium mixture of variable composition.

3. Addition of hydrogen chloride to the arsine/hydrogen line both to add
hydrogen chloride to the reactant gas mixture downstream of the gallium to de-
termine its effect on growth rate, background carrier concentration, etc., and
also to etch clean the reactor tube and substrate holder prior to a deposition
run.

4. Addition to n-type doping gases such as hydrogen sulfide, hydrogen
selenide, or hydrogen telluride.

5. Inclusion of a line for addition of other doping materials such as
diethylzinc to allow p-type doping.

6. An ability to introduce chlorine into the "chromium" doping line. The
introduction of metallic chromium or iron into the chromium feed tube of the
reactor permits the addition of the respective metallic chlorides into the

6

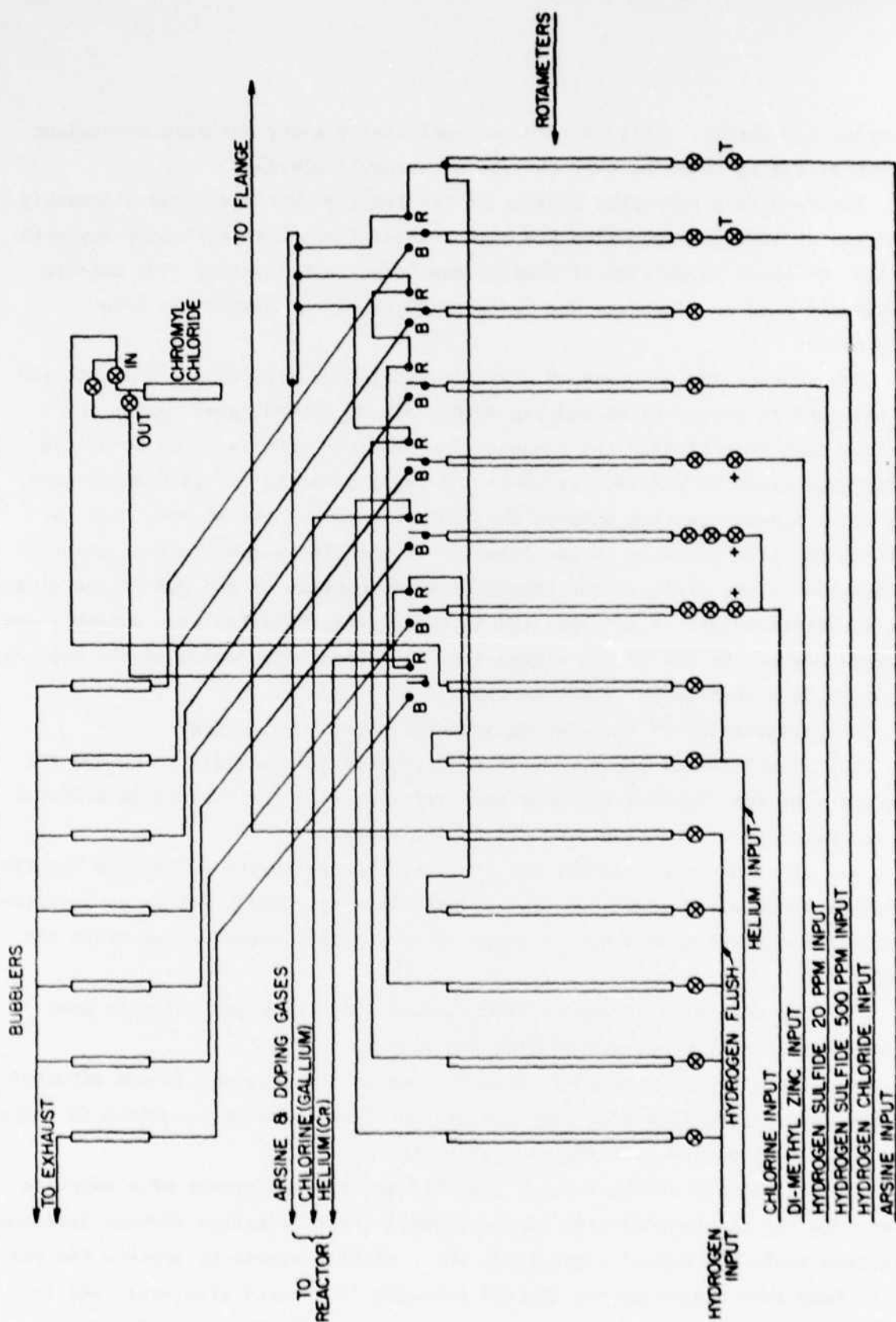GALLIUM ARSENIDE VAPOR PHASE GAS SYSTEM

Figure 2. Schematic diagram of reactor gas-handling system.

7

reacting gas stream. This could be a considerably safer and more convenient method of adding chromium than the use of chromyl chloride.

Figure 3 is a schematic diagram of the reactor tube and furnace assembly. The reactor tube configuration has been changed from that previously employed at RCA for vapor deposition of GaAs by the $Ga/HCl/AsH_3$ system. The sidearm previously used to discharge the waste products of the system has been eliminated.

The reactor now consists of a single straight quartz tube. The exit end of the tube is closed by an end cap with a sleeve extending so far up the reactor tube that sliding the furnace down the tube permits it to be heated and etched clean of reaction products. A small quantity of hydrogen or nitrogen flows slowly upstream between the reactor tube and the sleeve; this restricts reaction products to the interior of the sleeve and prevents their deposition on the walls of the reactor tube downstream of the end of the sleeve. The substrate holder is incorporated in the end-cap holder-sleeve assembly and extends beyond the end of the sleeve into the deposition region of the reactor. Figure 4 is a photograph of the reactor.

The elimination of the sidearm achieves several objectives:

1. It eliminates the necessity to dismantle the assembly to remove the reactor tube for cleaning whenever the performance of the reactor is affected by the deposits of reaction products in the sidearm.

2. It reduces the history effect (i.e., change in the background impurity level produced after growth of highly doped layers). This feature is important when attempting to grow a buffer layer after a highly doped device wafer has been grown.

3. The reactor tube can be etch cleaned (with hydrogen chloride gas) before every run without dismantling the system.

4. The gas flow pattern is uniform down to the tube and is not affected by the reverse gas flow from the loading end of the reactor, required to force the reaction products down the side exit arm.

Other features of the reactor assembly are the employment of a sapphire feed tube for the introduction of the chromyl chloride/helium mixture into the reaction zone, the use of a pyrolytic boron nitride sleeve to protect the reactor tube from attack by the chromyl chloride in the reaction zone, and the employment of an annular heat pipe using sodium as the heat transfer medium, as a heating device for the deposition zone.
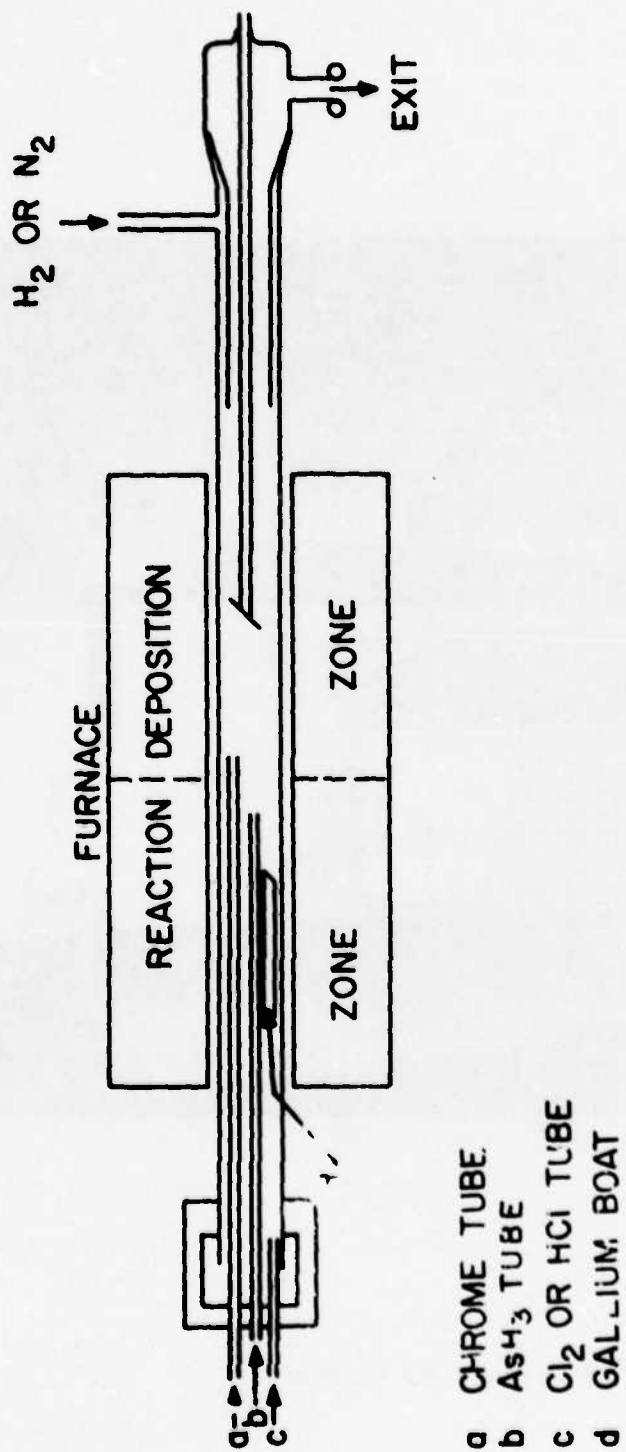
8

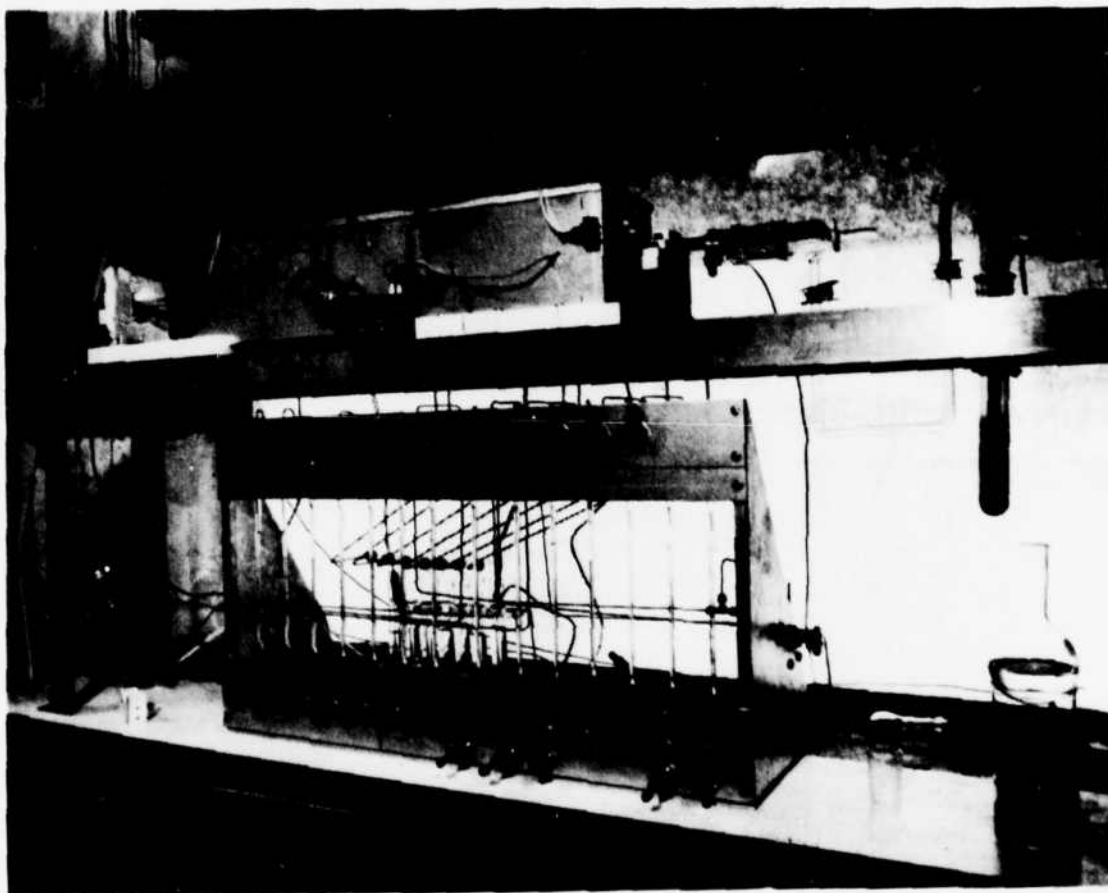Figure 3. Schematic diagram of reactor tube/furnace assembly.

Figure 4. Photograph of reactor.

10

C. RESULTS

1. Undoped High-Resistivity Layers

The reactor has been fabricated and is now operational. As discussed earlier, to obtain Cr-doped epitaxial SI layers, it is necessary to ensure that the reactor background is n type, and $(N_D - N_A)$ is less than 2×10^{15} cm^{-3}. The initial wafers grown in the reactor were found to be of high resistivity even in the absence of added Cr. The reactor was completely leak checked to ensure that there was no oxygen or moisture present. Epitaxial layers were again grown on SI GaAs substrates. The epitaxial layers were found to be of high resistivity with $\rho > 3 \times 10^4$ ohm-cm at 300 K. The resistivity at 77 K was too high to measure. This indicates that the high resistivity is due to some deep level or levels. A sample was sent to our analysis group for evaluation by SIMS to determine whether it is due to a specific dopant or caused by defects. This test was inconclusive.

The occurrence of high-resistivity background layers during growth on high-resistivity substrates has been noticed before [3]. The experiments of Cox and DiLorenzo [3] indicate that this is due to the diffusion of acceptors from the substrate or the substrate-epi layer interface. In fact, Cox and DiLorenzo utilize this high-resistivity layer as a buffer layer for FETs [3]. We have observed such layers previously with the AsH$_3$/Ga/Cl$_2$ process. The nature of the acceptors is not known; it is suspected that they are point defects.

Attempts to characterize these undoped layers by the usual Van der Pauw methods have been made. Resistivities of the order of $4-5 \times 10^4$ ohm-cm have been measured. Attempts to determine carrier concentration from these experiments have failed due to insufficient equipment sensitivity. However, with substrate/epi-layer thickness ratios of approximately 10 to 21, measurements are strongly influenced by the presence of the substrate.

A rough method, adopted for assessing the breakdown voltage of the epi layers, is as follows: Two tungsten wire probes are pressed onto the surface of the epi layer, spaced approximately 0.25 cm apart, and a voltage is applied between them by means of a curve tracer. This gives an I/V curve and shows the voltage breakdown of the material, if any. Good buffer layers will

11

withstand up to 1500 V, the maximum capability of the instrument. Figure 5 shows traces produced by wafers A94 and A95.

2. Chromium-Doped Layers

The original method selected to attempt chromium doping was to bubble a carrier gas (helium) through liquid chromyl chloride. Because of a suspected leak in this part of the system, we are currently using a 500-ppm mixture of chromyl chloride (CrO_2Cl_2) in helium prepared in cylinders by Airco Precision Gas Co.[*]

Several chromium-doping runs have been made. Typical curve-tracer breakdown photographs are shown in Fig. 6 (wafers 89, 92, and 96). Attempts to measure the chromium content of these epitaxial layers by SIMS have been unsuccessful. We have sent several thick epi layers for evaluation by spark-source mass spectroscopy (SSMS). We will attempt using a weak spark and moving the wafer under the spark to limit erosion to less than 5 μm. This should prevent the substrate from influencing the measurement.

In Fig. 6, note that a dopant flow of 500 ml/min of CrO_2Cl_2 (500 ppm) produces a higher resistivity than does a flow of 275 ml/min. When the flow was increased to 1000 ml/min, the layer reverted to n type with mid-10^{14} cm^{-3} carrier concentration.

The surface morphology of Cr-doped epi layers grown in the modified reactor is excellent. This is in contrast to the layers grown in our older reactor. The precise reason for the dramatic improvement in surface morphology is not known.

3. Device Wafers

As the object of growing semi-insulating layers on SI GaAs substrates is to provide a superior surface for the growth of device wafers, a number of wafers suitable for GaAs FET fabrication have been grown. These have either a 12-μm-thick undoped high-resistivity layer or a chrome-doped layer, followed by the n and n^+ layers needed for FET fabrication. These wafers are A63, A67, A73, and A73 with undoped buffer layers, and A69 with a chrome-doped buffer layer. Figure 7 shows the carrier-concentration profile of wafer A69.

---

[*]Riverton, NJ.
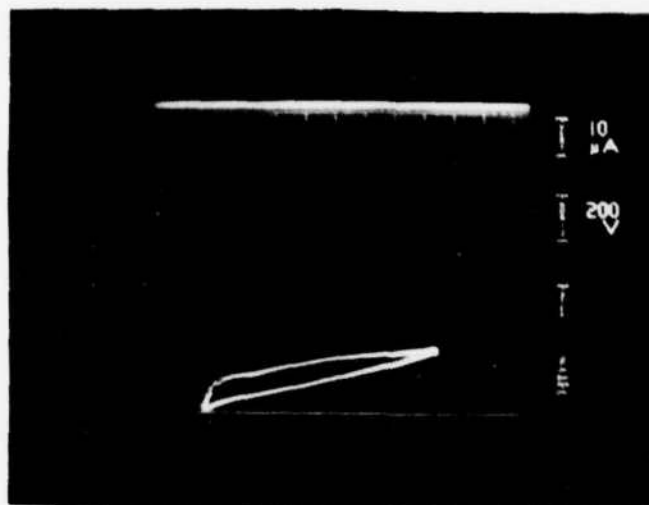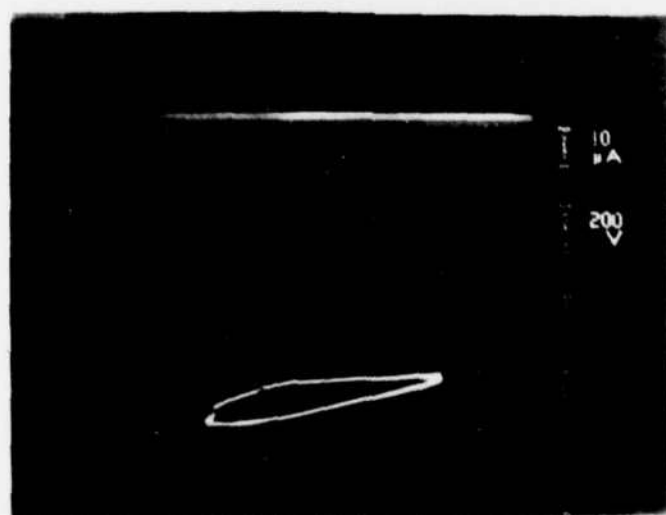
Figure 5. Two-point probe characteristic of undoped layers.

13

A89

Dopant flow:
600 ml/min.

A92

Dopant flow:
275 ml/min.

A96

Dopant flow:
500 ml/min.

Figure 6. Two-point-probe data for Cr-doped epi layers.
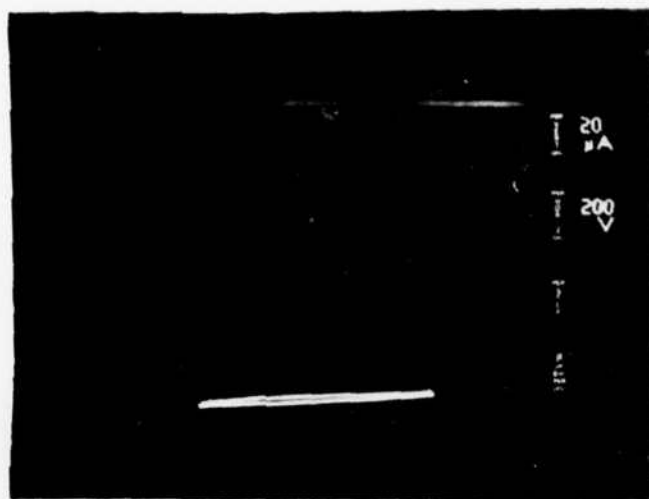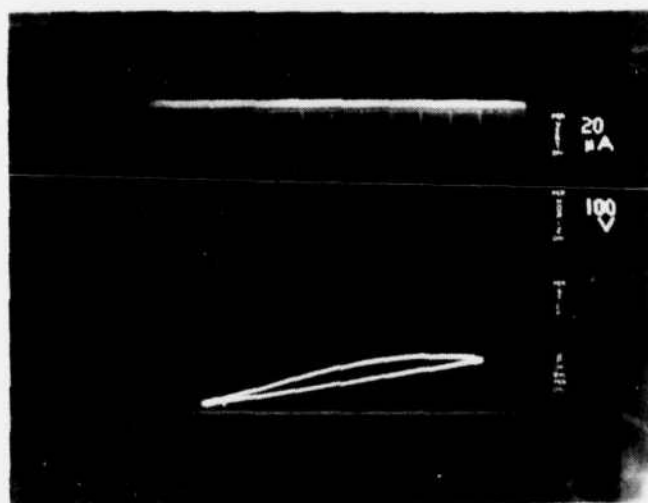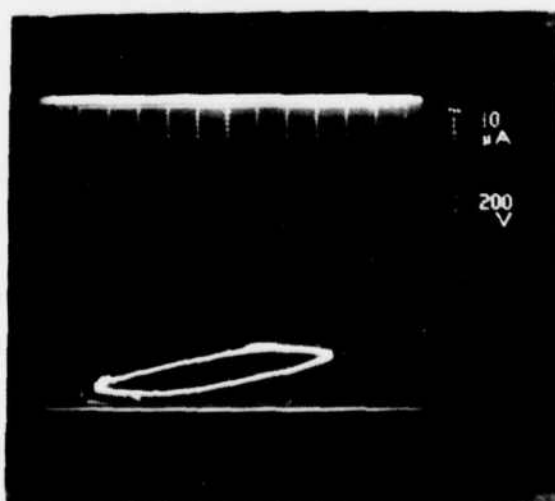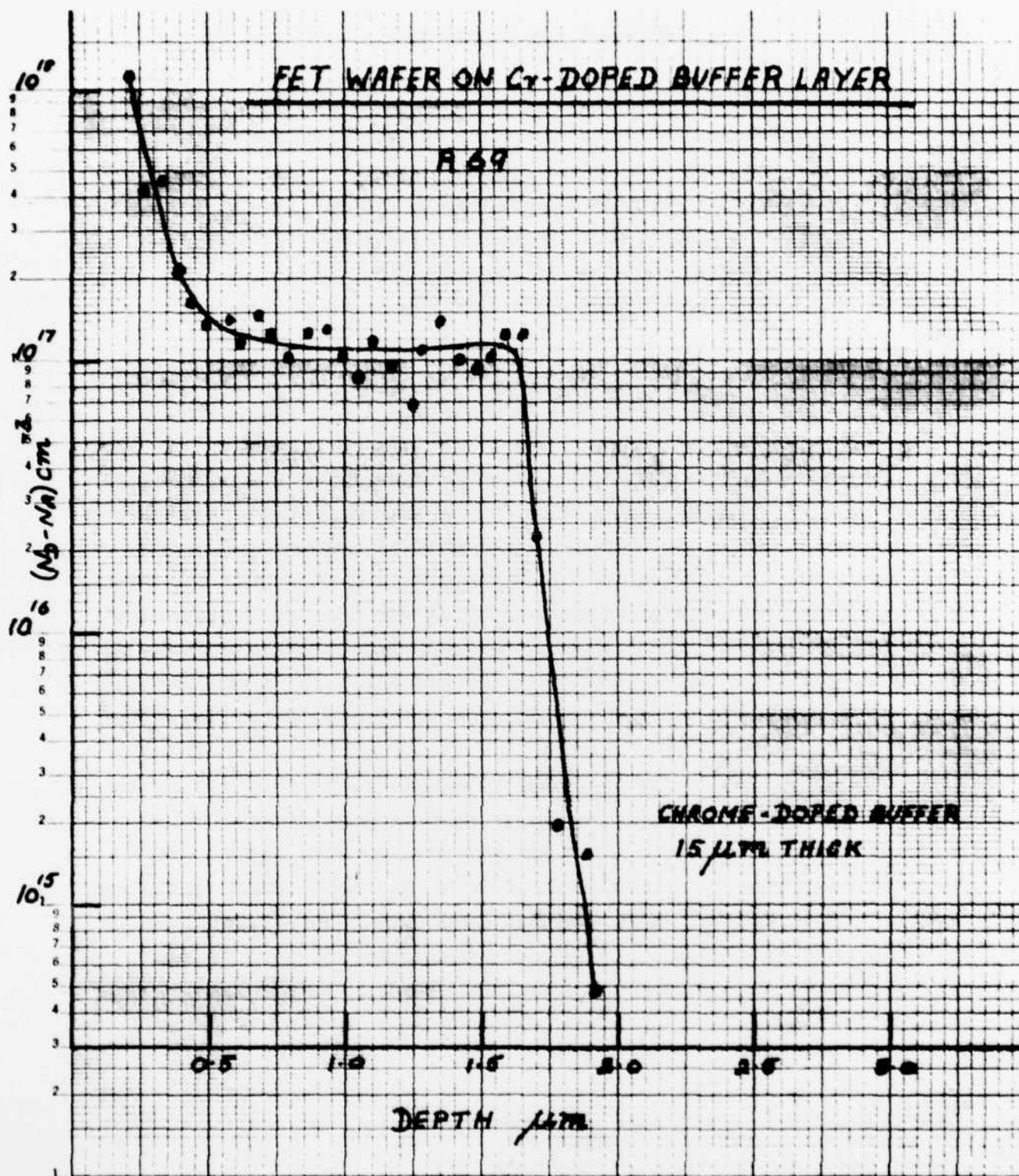
14

Figure 7. Carrier-concentration profile of wafer A69.

SECTION III

MATERIAL CHARACTERIZATION

Detection and identification of deep levels in SI GaAs is an important
step toward characterization of the material. Cr and O are the two most
common elements producing deep states, although material that is somewhat
more insulating has been obtained of late with Cr doping. Even at satura-
tion, the Cr concentration in GaAs remains at the parts-per-million level,
making analytical detection of the element difficult. To date we have found
that only spark-source mass spectrometry (SSMS) has reliably detected Cr in
GaAs.

However, it has been known for some time [4-6] that transitions to and/
or from Cr acceptors in SI GaAs could be excited optically with a photon
energy of about 0.9 eV. It is not clear in the literature whether holes or
electrons are responsible for the increased photoconduction with this subgap
illumination, although this could be determined with a photo-Hall experiment.
Nevertheless, a peak in the photoconductive spectral response at 0.9 eV
would appear to be the "signature" of Cr presence in the lattice. The results
of preliminary, room-temperature measurements to test the use of photoconduc-
tivity for detection of Cr in currently used substrate material are shown in
Fig. 8. Here the conductivity per μW of incident radiation (normalized photo-
conductivity) for three types of SI substrates is shown as a function of the
photon energy.

The Sumitomo[*] oxygen-doped substrate served as a control in the experi-
ment. The PC response of this material is somewhat featureless at 0.9 eV,
as expected. The Morgan[**] substrate did show evidence of a peak at 0.9 eV.
SSMS determined that the concentration of Cr in this sample was about 0.1 ppm
$(2x10^{15} cm^{-3})$. The Laser Diode[+] material exhibits a definite peak at 0.9 EV
and was determined, by SSMS, to have a Cr concentration of about 1.1 ppm
$(2.3x10^{16} cm^{-3})$. In addition, the Laser Diode material showed lower dark

---

[*]Sumitomo Electric Industries, Ltd., Osaka, Japan.
[**]Morgan Semiconductor Inc., Garland, TX
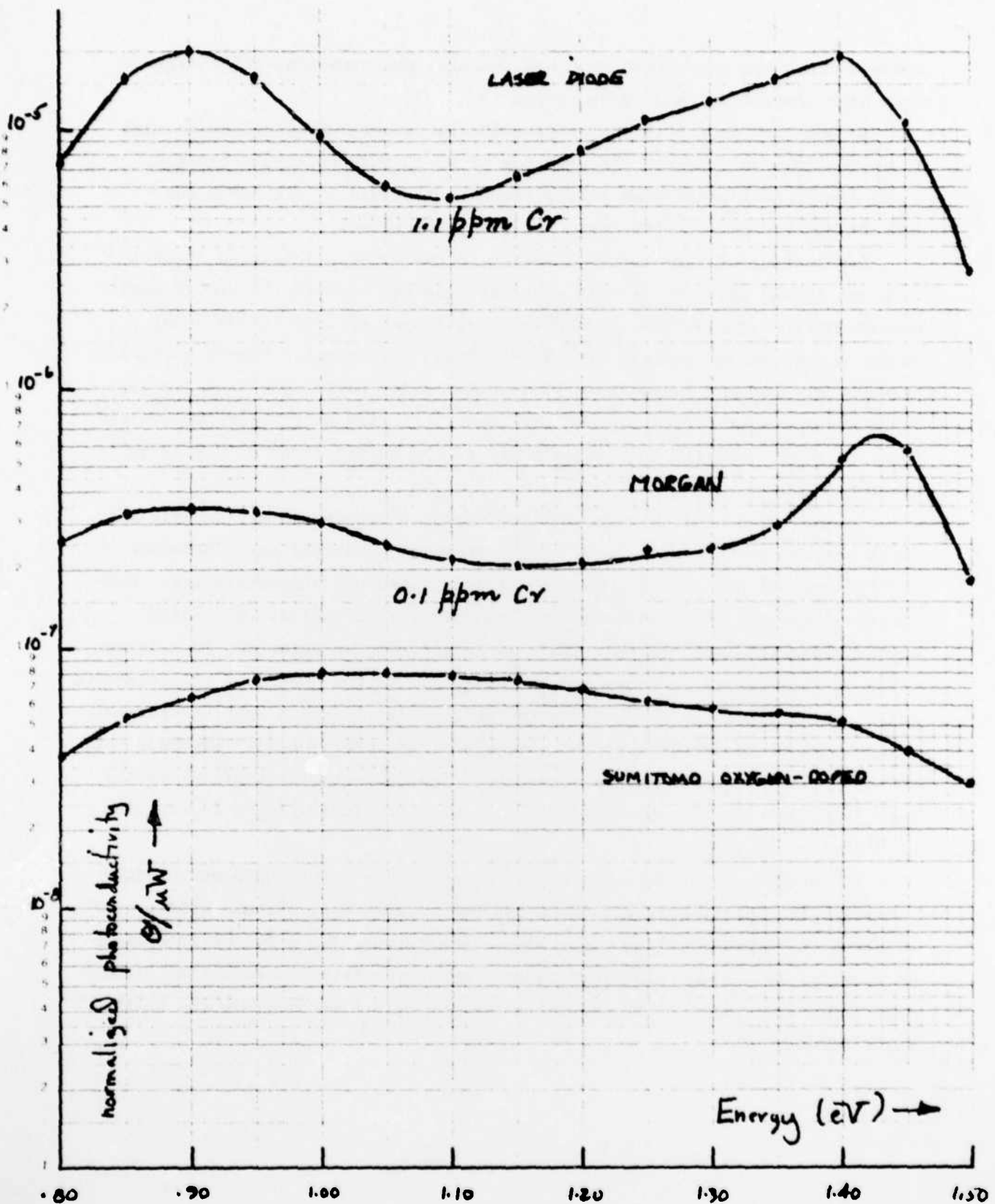[+]Laser Diode Laboratories, Inc., Metuchen, NJ.

16

Figure 8. Room-temperature photoconductivity response of SI GaAs substrate.
Note evolution of a peak at ~0.9 eV as Cr content increases.

conductivity than the Morgan, and had the slow photoresponse characteristic of a high concentration of deep traps.

We conclude from this that photoconductivity measurements can be used to nondestructively detect the presence of Cr in GaAs substrate material. It is likely that other deep states could be resolved by extending the measurement to lower temperatures and photon energies.

Application of this method directly to the in situ detection of Cr in thin epi layers grown on SI GaAs substrates is not straightforward, however. Measurements of the optical absorption coefficient of Cr-doped material showed a negligible increase at 0.9 eV. Thus, the material remains optically transparent, and any increase in photoconductivity could come from the Cr-doped substrate as well as the buffer layer. In view of the relative thickness, it seems unlikely that the effects of the buffer layer at 0.9 eV would be seen at all.

On the other hand, band-edge illumination is absorbed very rapidly with depth because of the large value of the absorption coefficient. Behavior of the PC spectral response for the substrates tested was always similar. Conduction increased near the band edge and then dropped off as the photon energy increased (see Fig. 8). This is interpreted as being due to a large value of the surface recombination velocity S. As the generated hole-electron pairs are confined to the surface, the photoconductivity is seen to decrease. Figure 9 shows the results of the same experiment (PC spectral response) for two SI epi films on the Morgan substrate. The characteristic dip above the band edge seen for the substrate was not observed, indicating a lower value of S in the epi material.

The usefulness of photoelectronic measurements with subgap and bandgap radiation in characterizing GaAs:Cr has become apparent. Future effort will be directed toward lowering measurement temperatures for a better resolution of deep levels. Also, photoluminescence measurements with excitation greater than the energy gap will be attempted for the detection of Cr in the buffer layer alone.
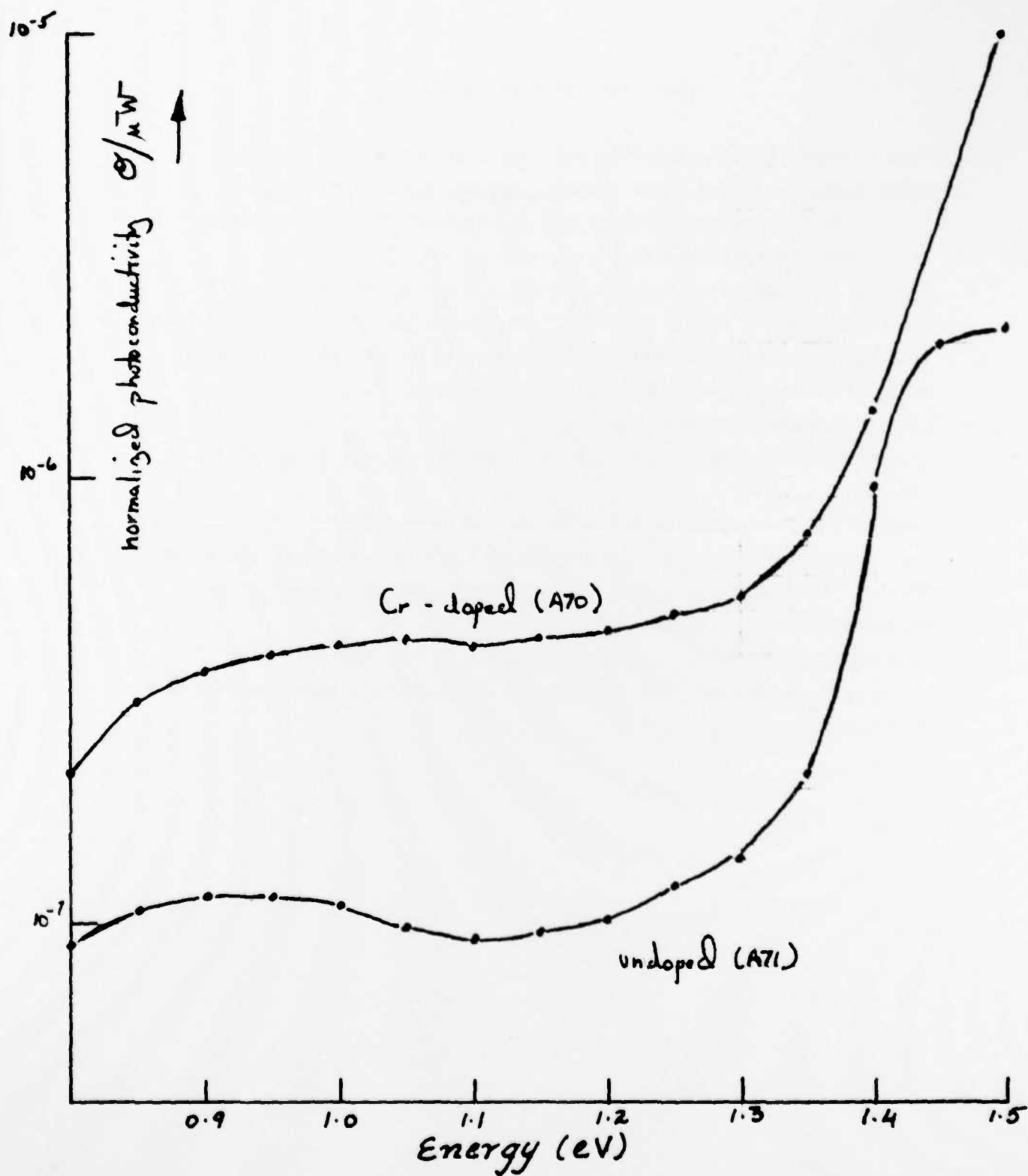
18

Figure 9. Room-temperature PC spectral response of two
epi SI films on Morgan SI substrate.

19

SECTION IV

PLANS FOR THE NEXT INTERVAL

1. Grow Cr-doped high-resistivity epi layers on a variety of SI GaAs substrates, including those showing thermal conversion. The objective is to determine whether the development of this technology will relax the specifications on substrate material.

2. Study ion implantation into Cr-doped epi layers. We will investigate implantation of ^{32}S and ^{28}Si. The properties of layers implanted into epi layers (μ, activation efficiency) will be compared to those of layers directly implanted into SI GaAs substrates.

3. Continue photoconductivity studies.

4. Try photo-Hall measurements on both Cr-doped epi layers and SI substrates.

5. Measure resistivity of Cr-doped epi layers as a function of temperature.

6. Grow thin n layers on SI GaAs substrates with, and without, epi buffer layers. Investigate traps at the n-layer interface to assess the efficacy of the buffer layer.

7. Grow TELD and FET wafers with Cr-doped epi buffer layers.

8. Investigate possibility of analysis of chrome-doped layers using spark-emission spectroscopy.

20

REFERENCES

1. H. C. Huang et al., "GaAs MESFET Performance," *IEDM Dig.*, 1975,
    pp. 235-257.

2. A. Shibatomi et al., "Characterization of Interface Region in VPE GaAs,"
    JCG Proc. Third Int. Conf. Vapor Growth and Epitaxy, Aug. 1975.

3. H. M. Cox and J. V. DiLorenzo, "Characteristics of an $AsCl_3/Ga/H_2$
    Two-Bubbler GaAs CVD System for MESFET Applications,"
    Proc. Sixth Int. Symp. GaAs and Related Compounds; Inst. Phys.
    Conf. Series, No. 336, London, 1977, pp. 11-22.

4. D. R. Heath, P. R. Selway, and C. C. Tooke, "Photoconductivity and
    Infra-red Quenching in Chromium-doped Semi-insulating Gallium Arsenide,"
    Brit. *J. Appl. Phys. (J. Phys. D)* $\underline{1}$ (Ser. 2), 29 (1968).

5. W. Plesiewicz, "Photoelectronic Investigations of Semi-Insulating p-Type
    GaAs:Cr Containing Neutral Chromium Acceptors," *J. Phys. Chem. Solids*
    $\underline{38}$, 1079 (1977).

6. H. J. Stocker, "A Study of Deep Impurity Levels in GaAs Due to Cr and O
    by AC Photoconductivity," *J. Appl. Phys.* $\underline{48}$, 4583 (1977).

DISTRIBUTION LIST

TECHNICAL REPORT

Contract N00014-77-C-0542

	number of copies
Program Management Defense Advanced Research Projects Agency Architect Building 1400 Wilson Blvd. Arlington, VA 22209	2
Code 427 Office of Naval Research Arlington, VA 22217	3
Naval Research Laboratory 4555 Overlook Avenue S.W. Washington, D. C. 20375 Code 5220 Code 5270	1 1
Defense Documentation Center Building 5, Cameron Station Alexandria, VA 22314	12
ONR Boston 495 Summer Street Boston, Massachusetts 02210	1
TACTEC Battelle Memorial Institute 505 King Avenue Columbus, Ohio 43201	1
Dr. Y. S. Park AFAL/DHR Building 450 Wright-Patterson AFB, OH 45433	1
ERADCOM DELET-M Fort Monmouth, N.J. 07703	1
Texas Instruments M. S. 105 P. O. Box 5936 Dallas, Texas 75222	1

Mr. H. Cooke   1
Avantek, Inc.
3175 Bowers Avenue
Santa Clara, CA 95051

Mr. R. Bell, K 101   1
Varian Associates
611 Hansen Way
Palo Alto, CA 94304

Mr. R. Bierig   1
Raytheon Company
28 Seyon Street
Walthon, MA 02154

Mr. H. C. Nathanson   1
Westinghouse R&D Center
Beulah Road
Pittsburgh, Pennsylvania 15235

Dr. F. Blum   1
Rockwell International Science Center
P. O. Box 1085
Thousand Oaks, CA 91360

Mr. G. J. Gilbert   1
MSC
100 Schoolhouse Road
Somerset, New Jersey 08873

Mr. C. Krumn   1
Hughes Research Laboratory
3011 Malibu Canyon Road
Malibu, California 90265

Mr. Hunter Chilton   1
RADC/OCTE
Griffiss AFB NY 13441

Mr. Lothar Wandinger   1
ECOM/AMSEL/TL/IJ
Fort Monmouth, NJ 07003

Colonel Paul Mosteller   1
AFOSR/NE, Bldg 410
Bolling AFB Wash DC 20375

Dr. Harry Wieder   1
Naval Electronics Laboratory Center
Code 922
271 Catalina Blvd
San Diego, CA 92152

23

Dr. William Lindley
MIT
Lincoln Laboratory
E124A P. O. Box 73
Lexington, MA   02173

Mr. Sven Roosild
AFCRL/LQD
Hanscom AFB, MA   01731

Mr. John Kennedy
AFCRL/LQP
Hanscom AFB, MA   01731

Mr. Don Reynolds
AFAL/DHR
Wright-Patterson AFB, OH 45433

Mr. John Carroll
RADC/RBRP
Griffiss AFB, NY   13441

Dr. Robert Thomas
RADC/RBRM
Griffiss AFB, NY 13441